Analytical relation of band gaps to both chirality and diameter of single-wall carbon nanotubes

J. W. Ding,[1,2,*] X. H. Yan,[1] and J. X. Cao[1,2]

[1]*Department of Physics, Xiangtan University, Xiangtan 411105, Hunan, China*
[2]*Institute of Mechanics and Material Engineering, Xiangtan University, Xiangtan 411105, Hunan, China*
(Received 22 April 2002; published 1 August 2002)

We present a tight-binding model of single-wall carbon nanotubes with curvature-modified hopping parameter γ_i, from which an analytical relation of band gaps to both chirality and diameter is derived by developing a transfer matrix method. The results are in agreement with the experimental results obtained from scanning tunneling microscopy and scanning tunneling spectroscopy measurements by three groups.

As a simple one-dimensional nanoscaled structure, single-wall carbon nanotubes (SWCN's) have been the subject of intensive theoretical and experimental efforts because of their singular properties and potential applications.[1–6] To understand the properties of SWCN's, theoretical simulations often focus on their electronic band structures.[7–17] It is found that depending on their diameter and chirality, SWNT's with various band gaps may be an insulator, a semiconductor, or a metal. Profoundly, a semiconducting SWCN has a primary band gap E_g, which is inversely proportional to its tube diameter d,[9–11] while a chiral metallic SWCN as well as a metallic zigzag tube is predicted to have narrow-gap scaling by $E_g \propto 1/d^2$.[12] These results are so interesting as to be similar to those measured by experiments.[18–20] Due to the curvature effect, however, it is argued[17] that the band gap of a semiconducting SWCN consists of two parts E_0 and E_θ, of which the main term E_0 is only dependent on diameter but the correctional term E_θ is dependent on both chirality and diameter. This may predict that the chirality of SWCN's should also modify their electronic structures. In this Brief Report, we present a tight-binding model of SWCN's with curvature-modified hopping parameters, from which an analytical expression of energy bands and gaps related to both diameter and chirality is derived by developing a transfer matrix method. The results are consistent with the experiments.

A (n,m) SWCN can be specified by its chiral vector $\mathbf{C}_h = n\mathbf{a}_1 + m\mathbf{a}_2$, where $\mathbf{a}_1$ and $\mathbf{a}_2$ are graphite primitive lattice vectors with $|\mathbf{a}_1| = |\mathbf{a}_2| = a$ as shown in Fig. 1. The tube diameter and the chirality are uniquely characterized by[1–3]

$$d = a(n^2 + m^2 + nm)^{1/2}/\pi, \tag{1}$$

$$\cos\theta = (n + m/2)/(n^2 + m^2 + nm)^{1/2}, \tag{2}$$

respectively. The translation vector $\mathbf{T}$, defined to be the unit vector of a SWCN, is parallel to the tube axis and normal to $\mathbf{C}_h$ in the unrolled graphite lattice in Fig. 1. In terms of $\mathbf{C}_h \cdot \mathbf{T} = 0$, the expression for $\mathbf{T}$ is given by

$$\mathbf{T} = \mathbf{a}_1(2m+n)/d_R - \mathbf{a}_2(2n+m)/d_R, \tag{3}$$

with $|\mathbf{T}| = T = \sqrt{3}\pi d/d_R$, where d_R is the greatest common divisor of $2m+n$ and $2n+m$. In a translatory unit cell, the number of hexagons, N, is obtained by

$$N = 2(n^2 + m^2 + nm)/d_R. \tag{4}$$

Associated with the periodic boundary conditions on $\mathbf{C}_h$, the wave vector $\mathbf{K}$ can be expressed by[3,7,9,10]

$$\mathbf{K} = \mu\mathbf{K}_1 + \frac{k}{|\mathbf{K}_2|}\mathbf{K}_2 \quad \left(\mu = 1,2,\ldots,N; -\frac{\pi}{T} < k < \frac{\pi}{T}\right), \tag{5}$$

where $|\mathbf{K}_1| = 2/d$ and $|\mathbf{K}_2| = 2\pi/T$ are the discrete unit wave vector in the circumferential direction and the reciprocal lattice vector along the tube axis, respectively.

To study the electronic properties of SWCN's, one usually adopts the nearest-neighboring tight-binding model with all on-site energies fixed at Fermi energy E_f.[7–9] As a simple physical scheme, hopping integrals γ_i were generally chosen to be an identical value γ_0 or added an additional averaging correction, while the variations in γ_i from bond to bond direction on $\mathbf{r}_i$ ($i=1,2,3$) were neglected.[3,7,9] Due to the curvature effect, however, the broken symmetry makes the variations in γ_i dependent on the geometrical structure of a SWCN, which plays an essential role in determining the electronic properties.[7,12,16,20] Following Ouyang *et al.*[20] but considering the anisotropy on direction $\mathbf{r}_i$, we assume that γ_i is reduced by a factor of $\cos\alpha_i$, where $\alpha_i = \frac{1}{2}\mathbf{K}_1 \cdot \mathbf{r}_i$ is the angle between two nearest-neighboring π-like electronic orbitals on the curved surface.[20] This situation brings some new difficulties in an analytical study of the properties of chiral SWCN's, because the minimum number of atoms in a translatory unit cell can be very large even for a relatively small-diameter chiral tube. For example, a (11,10) tube with a
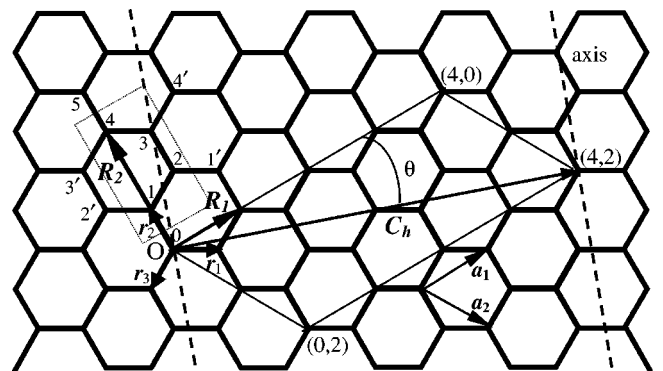

FIG. 1. The unrolled two-dimensional graphite sheet lattice of a (4,2) tube with a chiral angle θ. A four-carbon-atom unit cell is shown in the dotted rectangle. Dashed lines run in the direction of the tube axis.

radius ~ 0.7 nm contains 1324 carbon atoms in a translatory unit cell. In terms of the rotational and helical symmetry of a SWCN,[9] however, we need only consider a four-carbon-atom unit cell defined by the dotted rectangle in Fig. 1. The electronic wave functions at the atoms in this unit cell as well as their nearest neighbors are labeled as ψ_i and $\psi_{i'}$ ($i = 0,1, \ldots ,5$), respectively. To facilitate analysis of variations in electronic structure with chirality, a pair of orthogonal lattice vectors $\mathbf{R}_1 = \mathbf{a}_1$ and $\mathbf{R}_2 = \mathbf{a}_1 - 2\mathbf{a}_2$ have been introduced, as shown in Fig. 1.

Based on the Bloch theorem, the wave function ψ_i should satisfy that $\psi_{i'} = \lambda_1^{\pm 1} \psi_i$ and $\psi_{i+4} = \lambda_2 \psi_i$, where $\lambda_1 = e^{i\mathbf{K} \cdot \mathbf{R}_1}$ and $\lambda_2 = e^{i\mathbf{K} \cdot \mathbf{R}_2}$. The tight-binding Schrödinger equation for a unit cell along $\mathbf{R}_2$ can be written as the transfer matrix form

$$\begin{pmatrix} \psi_{i+4} \\ \psi_{i+3} \end{pmatrix} = \mathbf{M} \begin{pmatrix} \psi_i \\ \psi_{i-1} \end{pmatrix} = \lambda_2 \begin{pmatrix} \psi_i \\ \psi_{i-1} \end{pmatrix}, \qquad (6)$$

where the 2×2 transfer matrix $\mathbf{M} = \mathbf{M}_4 \mathbf{M}_3 \mathbf{M}_2 \mathbf{M}_1$ can be obtained by

$$\mathbf{M}_1 = \begin{pmatrix} \dfrac{E}{\lambda_1^{-1}\gamma_1 + \gamma_3} & \dfrac{-\gamma_2}{\lambda_1^{-1}\gamma_1 + \gamma_3} \\ 1 & 0 \end{pmatrix},$$

$$\mathbf{M}_2 = \begin{pmatrix} \dfrac{E}{\gamma_2} & \dfrac{\lambda_1\gamma_1 + \gamma_3}{-\gamma_2} \\ 1 & 0 \end{pmatrix},$$

$$\mathbf{M}_3 = \begin{pmatrix} \dfrac{E}{\gamma_1 + \lambda_1\gamma_3} & \dfrac{-\gamma_2}{\gamma_1 + \lambda_1\gamma_3} \\ 1 & 0 \end{pmatrix}, \qquad (7)$$

$$\mathbf{M}_4 = \begin{pmatrix} \dfrac{E}{\gamma_2} & \dfrac{\gamma_1 + \lambda_1^{-1}\gamma_3}{-\gamma_2} \\ 1 & 0 \end{pmatrix},$$

with energy E. By using the product of matrix, one obtains that $\det(\mathbf{M}) = e^{-2i\phi}$, where the phase factor ϕ is defined by

$$e^{i\phi} = (\lambda_1^{-1}\gamma_1^2 + \lambda_1\gamma_3^2 + 2\gamma_1\gamma_3)/\rho, \qquad (8)$$

with $\rho = \gamma_1^2 + \gamma_3^2 + 2\gamma_1\gamma_3 \cos\mathbf{K} \cdot \mathbf{R}_1$. When we multiply both sides of Eq. (6) by a factor of $e^{i\phi}$ and let $\mathbf{M}' = e^{i\phi}\mathbf{M}$ with $\det(\mathbf{M}') = 1$, the dispersion relation, yielding $\text{tr}(\mathbf{M}')/2 = \cos(\mathbf{K} \cdot \mathbf{R}_2 + \phi)$, can be obtained by

$$E = \pm \left\{ \sum_{i=1}^{3} \gamma_i^2 + 2\gamma_1\gamma_2 \cos\left[\frac{2\pi(n+2m)\mu}{d_R N} - \frac{nkT}{N}\right] \right.$$
$$+ 2\gamma_2\gamma_3 \cos\left[\frac{2\pi(n-m)\mu}{d_R N} + \frac{(n+m)kT}{N}\right]$$
$$\left. + 2\gamma_1\gamma_3 \cos\left[\frac{2\pi(2n+m)\mu}{d_R N} + \frac{mkT}{N}\right] \right\}^{1/2}, \qquad (9)$$

which is only related to the indices (n,m) with no requirement of knowing the screw axis vector[7] or the symmetry vector.[9]

When $n = m$, Eq. (9) is simplified as

$$E = \pm \gamma_1 \left(1 + 4t \cos\frac{\mu\pi}{n} \cos\frac{ka}{2} + 4t^2 \cos^2\frac{ka}{2}\right)^{1/2}, \qquad (10)$$

with $T = a$, $\gamma_2 = \gamma_3 > \gamma_1$ and $t = \gamma_2/\gamma_1 > 1$, which corresponds to the dispersion relation of an armchair tube. From Eq. (10), a zero-energy gap $E_g = 0$ can be directly obtained, which shows that an armchair tube is stable against a Peierls distortion, consistent with the theoretical results[3,7,12] and experiments.[18–20] When $k = \pm \pi/a$, two von Hove singulities (vHS's) can be found at $E = \pm \gamma_1$ for any armchair tubes. However, their energy positions are dependent on tube diameter, which is at variance with those obtained by Saito et al.[21]

In the case of a zigzag $(n,0)$ tube, $T = \sqrt{3}a$ and $\gamma_1 = \gamma_3 < \gamma_2$, the dispersion relation may be directly obtained from Eq. (9) by

$$E = \pm \gamma_2 \left(1 + 4t \cos\frac{\mu\pi}{n} \cos\frac{\sqrt{3}ka}{2} + 4t^2 \cos^2\frac{\mu\pi}{n}\right)^{1/2}, \qquad (11)$$

with $t = \gamma_1/\gamma_2 < 1$, from which the energy gap is accurately given by

$$E_g = 2\gamma_2 \left|1 - 2t \cos\left(\frac{\pi}{3} - \frac{qa}{3d}\right)\right|, \qquad (12)$$

where $q = 0, \pm 1$ is the remainder of n divided by 3. Obviously, a curvature-induced gap appears in what were once believed to be metallic nanotubes ($q = 0$), which have been observed experimentally.[20] Under consideration of $\gamma_2 = \gamma_0$, $\gamma_1 = \gamma_0 \cos(\pi/2n)$ and $\pi d = \sqrt{3}na$, this type of gap is expressed as

$$E_g = 4\gamma_0 \sin^2\frac{\sqrt{3}a_{cc}}{4d}, \qquad (13)$$

with $a_{cc} = a/\sqrt{3}$ the C-C bond distance. For a large value of d, Eq. (13) can be approximated by $E_g = A_0/d^2$ with $A_0 = 3\gamma_0 a_{cc}^2/4$, which has the same scaling as that given by Ouyang et al.[20] Also, if one considers only an average correction for the curvature effect (i.e., $\gamma_1 = \gamma_2 = \gamma_3 < \gamma_0$, and thus $t = 1$), there would appear no energy gap. This means that the variations in γ_i should be considered in determining the electronic structure of SWCN's. Likewise, the band gaps of semiconducting zigzag tubes ($q = \pm 1$) can also be approximately given from Eq. (12) by

$$E_g = \frac{2\gamma_0 a_{cc}}{d} - \frac{13q\gamma_0 a_{cc}^2}{12d^2}. \qquad (14)$$

Neglecting the higher-order term, Eq. (14) shows the dependence of E_g on the reciprocal tube diameter d^{-1}, i.e., $E_g = 2\gamma_0 a_{cc}/d$, consistent with the previous results under a linear $\mathbf{k}$ approximation.[9–11] Due to the curvature effect, however, the correction of the higher-order term to E_g is more than 3 times that in the case of not considering curvature effect,[21] which allows proposing a different classification for semiconducting zigzag tubes ($q = \pm 1$) as that given by Yorikawa et al.[17] Also, the values of E_g predicted by the present model is in good agreement with those obtained from a sp^3 model[14] and a sp^3s^* model[15] for several semiconducting tubes, which means that the variations in γ_i from the bond to bond direction may be of equal or greater impor-
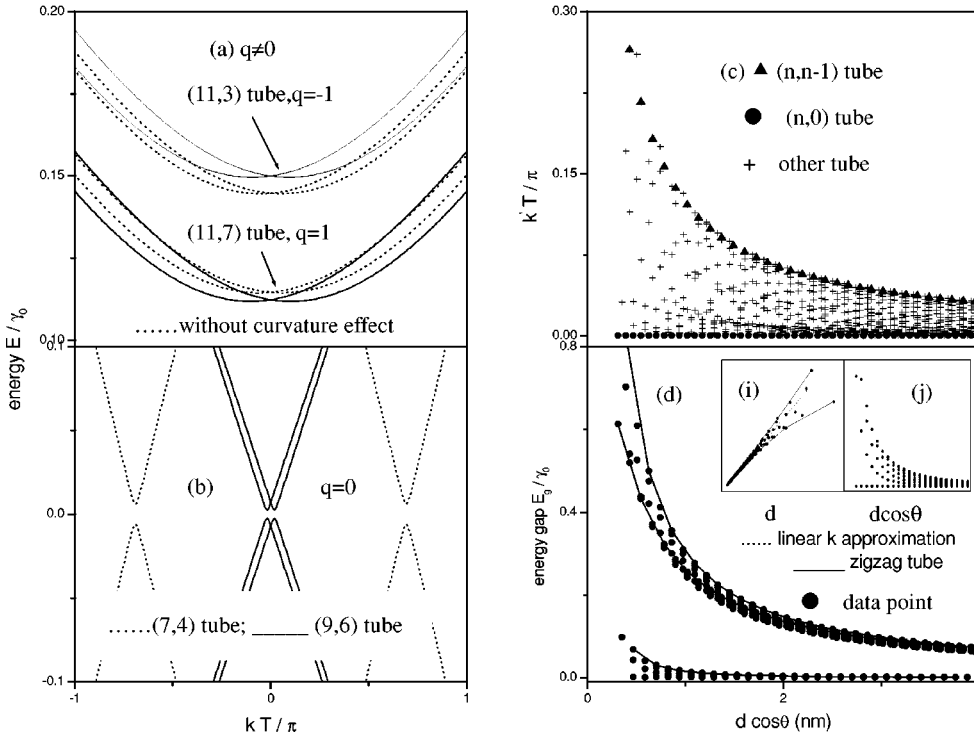
FIG. 2. The calculated band structures and energy gaps of chiral tubes ($4 \leqslant m \leqslant n \leqslant 50$).

tance than other curvature effects such as small s-p hybridizations in a SWCN. Additionally, in the case of a doubly infinite zigzag ($2n$,0) tube, whether semiconducting or metallic, there exist two vHS's at the same position of energy $E = \pm \gamma_0$, independent of both the diameter and curvature effect. This situation may provide a feasible way to obtain an accurate value of γ_0 from scanning tunneling spectroscopy (STS) experiments.

Neglecting curvature effects, i.e., $\gamma_i = \gamma_0$ ($i = 1,2,3$), Eq. (9) is further simplified by

$$E = \pm \gamma_0 \left[1 + 4 \cos\left(\frac{2n+m}{d_R N} \mu\pi + \frac{mkT}{2N} \right) \cos\left(\frac{3m\mu\pi}{d_R N} \right. \right.$$
$$\left. \left. - \frac{2n+m}{2N} kT \right) + 4 \cos^2\left(\frac{2n+m}{d_R N} \mu\pi + \frac{mkT}{2N} \right) \right]^{1/2}. \quad (15)$$

A straightforward relation of band gaps to the diameter and chirality of SWNT's with a larger tube diameter can be approximately obtained from Eq. (15) by

$$E_g = \frac{2|q|\gamma_0 a_{cc}}{d \cos \theta} - \frac{q\gamma_0 a_{cc}^2}{3d^2 \cos^2 \theta}, \quad (16)$$

with $\pi d \cos \theta = (2n+m)a/2$, where $n-m=3p+q$ with $q = 0, \pm 1$. It is clearly shown from Eq. (16) that the semiconducting energy gap is dependent on both diameter and chirality. Even neglecting the higher-order term in Eq. (16), the leading term still contains the factor of chirality, which can lead to a larger correction to E_g. In fact, WildÖer et al.[19] measured the energy gaps of several nanotubes with different chirality at $d = 1.4$ nm, ranging from 0.5 to 0.6 eV. However, it is a pity that the dependence of E_g on the chirality is usually neglected in the interpretation of experimental data

to obtain the value of γ_0, which may be one of the reasons why there exists a significant difference in γ_0 determined by several different experiments, ranging from 2.45 to 2.90 eV.[18–20]

As for the most general case of chiral tubes with curvature effects, we need only consider the lowest-lying conduction band (LCB) and the highest-lying valence band (HVB) to obtain the energy gap, which can reduce the complicated calculation, especially for a chiral tube with a much larger N. It should be noted that as a graphite sheet is rolled into a nanotube, the point **K** in the Brillouin zone is folded into another point with wave vector[3]

$$\frac{2n+m}{3}\mathbf{K}_1 + \frac{m}{d_R}\mathbf{K}_2.$$

Thereby, let

$$\mu = (2n+m+q)/3, \quad (17)$$

$$k = m|\mathbf{K}_2|/d_R + k', \quad (18)$$

where k' is still a continuous k variable. A subband of the LCB and HVB is then determined from Eq. (9). Another symmetrical subband of the LCB and HVB can also be obtained provided that $\mu = (n-m-q)/3$ and $k = (n+m)|\mathbf{K}_2|/d_R + k'$. The energy gap of a nanotube can be easily obtained from its LCB and HVB. In Fig. 2, we depict the band structures (LCB and HVB) of several representative chiral tubes and the energy gaps of all tubes ($4 \leqslant m \leqslant n \leqslant 50$). First, the k values of the positions of energy gaps of chiral tubes are shifted from those of zigzag tubes ($k = 0$) and armchair tubes ($k = \pm 2\pi/3T$) as shown in Figs. 2(a)–2(c), which is contrary to the previous expectation.[3] The shifted distance k' is depicted in Fig. 2(c), which is depen-

dent on both diameter and chirality with a profile determined by the $(n, n-1)$ tube. Next, due to the effect of chirality and curvature, a negative or positive correction to the semiconducting energy gap E_g is clearly seen from Fig. 2(a), which may lead to a large deviation of energy gaps from the linear k approximations [see inset (i) in Fig. 2(d)]. This may be one of the reasons of the large discrepancies between theory and experiment.[18,19] Third, the plots in Fig. 2(d) identify three distinct families of tubes: (a) with semiconducting energy gaps approximately scaling as $\sim 1/d \cos \theta$, (b) with curvature-induced gaps approximately scaling as $\sim 1/d^2 \cos^2 \theta$ [shown in the expanded scale in the inset (j)], and (c) with a zero-energy gap (armchair tube), which provides a complete description of numerical data[3,7,9] and a theory method.[12] Also, the zigzag $(3p \pm 1, 0)$ tubes determine the region of the values of energy gaps of all types of semiconducting nanotubes, as predicted by Saito *et al.*[21] This result can provide a convenience to analyze the experimental data, since the diameter and chirality of the specific nanotubes studied by STS was not accurately known in almost all cases. Especially, two symmetrical energy values are found in the LCB of a chiral tube, which means that a chiral tube is a binary-energy-value semiconductor. So some new phenomena may be expected on chiral SWCN's such as a indirect transition of electrons in optical spectrum experiments.

As the band gaps, predicted within present model, are characterized by not only the diameter but also the chirality of nanotubes, it is appropriate for us to directly compare the theoretical results with the original experimental data obtained by three groups[18–20] for different types of nanotubes, which provides a way to check the validity of the present model. The experimentally measured and theoretically calculated band gaps are shown in Fig. 3. Good agreement between the theory and the experiments is seen and an identical value of γ_0 has been obtained of about 2.60 eV from different experiments. This result may help to illuminate the large deviations in γ_0 determined from different experiments.[18–20] Therefore, the correction for curvature effects is necessary to obtain a more accurate value of γ_0 in the interpretation of the STS experimental data.[21]
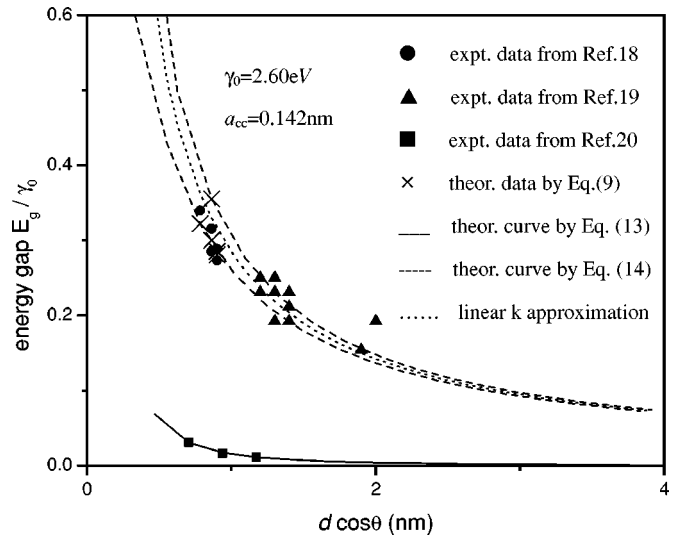

FIG. 3. The experimentally measured and theoretically calculated band gaps scaled by γ_0. The crosses correspond to the theoretical calculated gaps of the nanotubes measured by Odom *et al.* (Ref. 18).

In conclusion, we have studied the effect of chirality and curvature on electronic structures and energy gaps of SWCNs. The analytical results show that the band gaps depend on both the diameter and the chirality, which are consistent with experimental results. Because the diameter and chirality as well as the electronic structures of nanotubes can be directly determined by scanning tunneling microscopy (STM) and STS experiments, one may expect further confirmation of the present model approximation. These works have implications for our understanding of the electronic properties and potential applications of carbon nanotubes.

---

*Electronic address: jwding@xtu.edu.cn

[1] M. S. Dresselhaus, Nature (London) **391**, 19 (1998); Science **292**, 560 (2001).

[2] C. Dekker, Phys. Today **52**(2), 22 (1999).

[3] R. Saito, G. Dresselhaus, and M. S. Dresselhaus, *Physical Properties of Carbon Nanotubes* (Imperial College Press, Londom, 1998).

[4] P. G. Collins *et al.*, Science **292**, 708 (2001).

[5] R. R. Schlittler *et al.*, Science **292**, 1136 (2001).

[6] S. J. Tans *et al.* Nature (London) **393**, 49 (1998); R. Marter *et al.*, Appl. Phys. Lett. **73**, 2447 (1998).

[7] R. Saito *et al.*, Phys. Rev. B **46**, 1804 (1992).

[8] J. W. Mintmire, B. I. Dunlap, and C. T. White, Phys. Rev. Lett. **68**, 631 (1992).

[9] C. T. White, D. H. Rorbertson, and J. W. Mintmire, Phys. Rev. B **47**, 5485 (1993); C. T. White and T. N. Todorov, Nature (London) **393**, 240 (1998).

[10] R. Saito, G. Dresselhaus, and M. S. Dresselhaus, J. Appl. Phys.

73, 494 (1993); M. S. Dresselhaus, G. Dresselhauls, and R. Saito, Solid State Commun. **84**, 201 (1992).

[11] H. Ajiki and T. Ando, J. Phys. Soc. Jpn. **62**, 1255 (1993); **62**, 2470 (1993).

[12] C. L. Kane and E. J. Mele, Phys. Rev. Lett. **78**, 1932 (1997).

[13] N. Hamada *et al.*, Phys. Rev. Lett. **68**, 1579 (1992).

[14] X. Blase *et al.*, Phys. Rev. Lett. **72**, 1878 (1994).

[15] J. X. Cao, X. H. Yan, J. W. Ding, and D. L. Wang, J. Phys.: Condens. Matter **13**, L271 (2001).

[16] L. Yang and J. Han, Phys. Rev. Lett. **85**, 154 (2000).

[17] H. Yorikawa *et al.*, Phys. Rev. B **50**, 12 203 (1994).

[18] T. W. Odom *et al.*, Nature (London) **391**, 62 (1998); J. Phys. Chem. B **104**, 2749 (2000).

[19] J. W. G. Wildöer *et al.*, Nature (London) **391**, 59 (1998).

[20] M. Ouyang *et al.*, Science **292**, 702 (2001).

[21] R. Saito, G. Dresselhauls, and M. S. Dresselhaus, Phys. Rev. B **61**, 2981 (2000).